Advances in Military Technology
Vol. 19, No. 2, 2024, pp. 287-299
ISSN 1802-2308, eISSN 2533-4123
DOI 10.3849/aimt.01887

# Millimeter-Wave Radar Applicability for Increasing ZU-23 Firing Efficiency

V. Kudriashov[1], P. Open'ko[2*], M. Myroniuk[2], V. Voinov[3], D. Lytovchenko[3] and V. Khoma[2]

[1]*O.Ya. Usikov Institute for Radiophysics and Electronics of the National Academy of Sciences of Ukraine, Kharkiv, Ukraine*
[2]*The National Defence University of Ukraine, Kyiv, Ukraine*
[3]*Ivan Kozhedub Kharkiv National Air Force University, Kharkiv, Ukraine*

The manuscript was received on 8 February 2024 and was accepted after revision for publication as an original research article on 1 December 2024.

**Abstract:**

*The results of numerical modeling of air objects detection ranges using the paired ZU-23 anti-aircraft system and millimeter-wave (mm) radar in various combat conditions are presented to address the task of the improvement of air target engagement efficiency. Through extensive modelling, the effective scattering surface (ESS) of 23 mm projectile was determined. The slant ranges values to the firing zones far boundaries were found under various combat conditions. The probabilities of the ZU firing task fulfilment during autonomous actions and when the personnel work out the target designation (TD) from the mm wavelength range radar are calculated. The expediency of the mm wavelength range radars using for the TD formation on ZU is shown. The increment of shell firing efficiency due to the use of mm wavelength range radars is estimated. The obtained approximate expressions, shell firing efficiency indicators values and graphical material are presented.*

**Keywords:**

*detection range, detection probability, effective scattering surface, radar station, conditional probabilities of target engagement, increase in shooting efficiency*

## 1 Introduction

In the conditions of large-scale armed aggression by the Russian Federation against Ukraine, the enemy extensively apply Unmanned Aerial Vehicles (UAVs) to inflict damage, primarily targeting critical infrastructure objects. Considering such kind of

* *Corresponding author: Institute of Aviation and Air Defence, National Defence University of Ukraine, Air Force Avenue 28, UA-030 49 Kyiv, Ukraine. Phone: +38066 764 5920, E-mail: pavel.openko@ukr.net. ORCID 0000-0001-7777-5101.*

threats that operate at low and extremely low altitudes, anti-aircraft missile complexes are widely used in conjunction with anti-aircraft gun mounts (ZUMs) and standard small arms weaponry [1].

In this context, aerial targets like UAVs have significant characteristics and maneuvering capabilities that differ substantially from aerodynamic targets, especially in conditions of limited visibility or urban terrain. These differences necessitate enhancing their detection capabilities to ensure successful engagement. The small size of UAVs and their constant ability to change positions rapidly pose significant challenges for aiming anti-aircraft gun mounts (ZUMs), potentially leading to target misses. This, in turn, poses a threat to the lives and well-being of military personnel and civilian population within the range of bullets, specifically regarding the possibility of accidental bullet strikes or shrapnel injuries.

As a result, there is a need to implement millimeter-wave [mm] radar stations to enhance the effectiveness of target engagement using anti-aircraft gun mounts, while minimizing the risk to the lives and well-being of military personnel and civilians during enemy UAV attacks.

According to [1], the typical target (TT) for the ZU-23 anti-aircraft gun is the MiG-17 aircraft. Based on available data, when there is only notification (no target designation), the probability of missing the TT by personnel ($P$) at low altitudes is approximately 0.4, and at the altitudes of 2.5 km to 3 km, it is 0.8. Meanwhile, the statistical probability of detecting the TT ranges from only 0.6 to 0.2, respectively. The use of compact mm-wave radar systems [2, 3] for guiding the ZU-23 can address this deficiency.

The effectiveness of fire from a paired ZU-23 anti-aircraft gun is measured by the conditional probability of target engagement with $n$ shots $R_n$ [4, 5] and the probability of accomplishing the fire mission $P_{\mathrm{fm}}$. Based on the values of [4, 5], the increase in shooting effectiveness $\Delta_i$ and the applicability of using millimeter-wave radar systems are determined. The target detection and identification ranges depend on the background environment, target size, and color, meteorological visibility range (MVR), the firing position angular closure, and the optical interference presence. The same factors also affect the target acquisition range in the ZU collimator sight and the firing zone far boundary values.

### *1.1 Formulation of Problem*

The analysis of publications [1, 5, 6] showed that massive clouds with sharp transitions of dark and light areas underestimate the target detection range by the naked eye. The limitation in firing is due to the direction to the Sun no less than ±15°. Although, sun illumination from the opposite direction of firing increases target detection range $D_{\mathrm{d}i}$ and its identification. Target coloring can cause the target to blend in with the sky, effectively camouflaging it.

For example, coloring the target with silver aluminum color reduces $D_{\mathrm{d}i}$ up to 50 % of the white-grey background against a cloudless blue sky [1, 5]. Difficult meteorological conditions in the form of rain, fog and the use of aerosol (smoke) interference by the enemy are considered by lowering the MDV. For a target such as

the Su-7B, when the MDV is only 4 km, the naked eye can see up to 3.5 km. When the MDV is not less than 10 km $D_{di}$, the TT is ~6.8 km, when statistical probability of detection $P_{di}$ equals 0.5 [1, 5].

The combat performance quality of the personnel operating the ZU-23 is assessed on a scale from 'excellent' to 'satisfactory' and determines the values of the systematic errors in firing projectiles in the firing plane. The closure angles of the firing position (FP) do not always allow ZU personnel to engage targets promptly. Impulse and continuous optical interferences, as well as powerful jamming signals, can temporarily blind the personnel, preventing them from conducting fire. Signal rockets (projectiles, mines) and the traces of anti-aircraft guns complicate the process of detecting (and engaging) airborne targets [1, 6-10].

The aim of the article is to numerically model the range values and detection probabilities of air targets by ZU personnel and millimeter-wave radars, as well as the conditional engagement probabilities and slant ranges achievable at the distant boundaries of ZU firing zones (DBFZ), with the goal of improving the effectiveness of air target engagement. In order to prove the using of mm range radars applicability for guiding the ZU to the target, the firing task fulfillment probabilities are calculated as $R_{fm}$ and firing efficiency increments are determined as $\Delta_i$.

## 2 Description of the Method and Basic Mathematical Equations

**Determination of range values and probabilities of aerial targets detection**

We consider the ZU-23 firing at a TT and at a UAV. As a UAV we chose the 'Outpost' type vehicle. To assess the ZU firing effectiveness, we use the approximate largest $S_{max}$ and smallest $S_{min}$ target areas in the picture plane of projectile firing. We assumed for TTs $S_{max\,TT} = 30.2\ m^2$ and $S_{min\,TT} = 9.1\ m^2$, and for UAVs – $S_{max\,Out} = 6.7\ m^2$, $S_{min\,Out} = 0.58\ m^2$. The smallest $S_{min\,i}$ is expected when firing at low altitudes (angle of target location $\varepsilon \le 5^o$) and the largest $S_{max\,i} - \varepsilon > 45^o$. The average values of the TT flight speed and UAV respectively are equal to 250 m/s and 40 m/s.

The target detection ranges by ZU personnel, with a probability of correct detection of 0.5, can be determined using the following approximate expression [2, 4], depending on various factors:

$$D_d(S, \xi_c, \xi_m, \xi_p, \xi_s, K_c) = D_{TT} \sqrt{\frac{S}{S_{min\,TT}}}\, \xi_c\, \xi_m\, \xi_p\, \xi_s\, K_c \tag{1}$$

where $D_{TT}$ is the range of TT detection ( ~ 8.5 km [1]); $S$, $S_{min\,TT}$ is the target visualization area, on which the firing is conducted and TT is the smallest area in the picture area of firing, respectively; $\xi_c$, $\xi_m$ – respectively, the coefficients that take into account the coloring of the target ($\xi_c$ varies from 0.5 to 1) and MVR ($\xi_m$ varies from 0.48 to 1); $\xi_p$ – the coefficient that takes into account the quality of combat performance of the personnel of the ZU ('excellent' – 0.9; 'good' – 0.8; 'satisfactory' – 0.7; 'master' – 1.1); $\xi_s$ – the coefficient that takes into account the solar illumination of the target (is in the range from 1.3 to 1.5) [1]; $K_c$ – the

coefficient that takes into account the ZU closure angles (varies from 0 to 1, in modeling took 1).

The average target detection ranges with the naked eye $D_{TT}$ and acquisition in the ZU collimator sight, as determined through numerical modeling, were taken to be 8.5 km for moderately trained personnel that operate the ZU [2, 3].

The results of the calculations based on expression Eq. (1) are shown in Fig. 1.

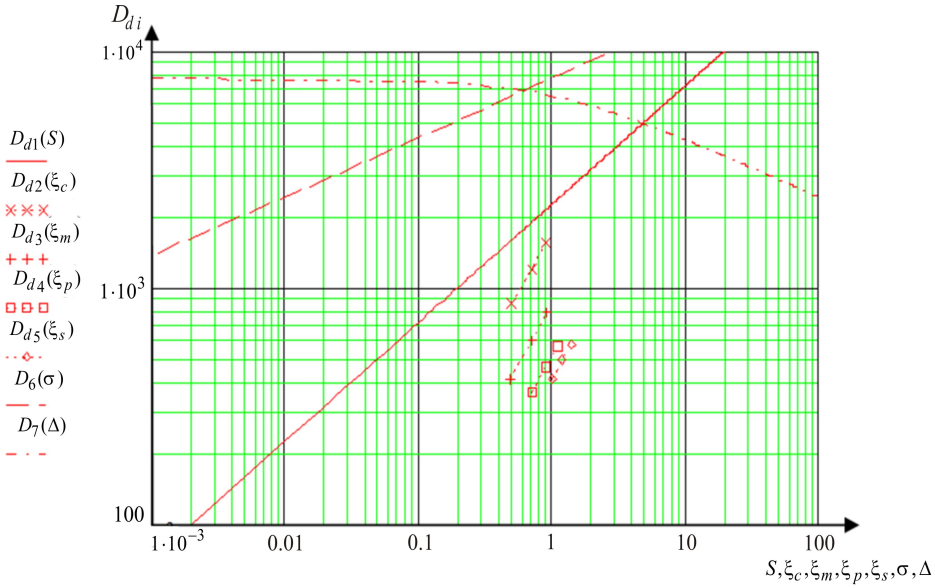


*Fig. 1 Target detection ranges $D_{di}$ under changing conditions $S$, $\xi_c$, $\xi_m$, $\xi_p$, $\xi_s$, $\sigma$ and $\Delta$*

The first straight line $D_{d1}(S)$ (indicated by a continuous line) represents the change in the range of target detection with a probability of 0.5, with the average trained personnel of the ZU ($\xi_p = 0.8$). The second ($\cdot\cdot\times\cdot\cdot\times\cdot\cdot$ $D_{d2}(\xi_c)$) and third ($\cdot\cdot+\cdot\cdot+\cdot\cdot$ $D_{d3}(\xi_m)$) straight lines give the detection range values of 'Outpost' type UAVs $S_{\min\,Out}$ under the effect of target color and MDV ($\xi_c = 0.5$), respectively. We observe a significant dependence of $D_d$ on the parameters $S$, $\xi_c$ and $\xi_m$ target. Straight fourth line ($\cdot\cdot\square\cdot\cdot\square\cdot\cdot$ $D_{d4}(\xi_p)$) is calculated considering the quality of the ZU personnel combat performance. The fifth straight line ($\cdot\cdot\lozenge\cdot\cdot\lozenge\cdot\cdot$ $D_{d5}(\xi_s)$) is obtained when there is the target solar illumination. Given the different target flight speed, the ZU personnel directional sounder cannot always fire at the far edge of firing zone. This leaves firing on a catch-up course.

The range of air targets detection $D_d(\sigma, \Delta)$ by small-size radar of mm wavelength range is calculated by the formula [1, 6, 9]:

$$D_d(\sigma,\Delta) = D_{TT}\sqrt[4]{[\sigma(q^2/2)]/[\sigma_{TT}(1+\Delta)\ (q_p^2/2)]}\ K_c \qquad (2)$$

where $D_{TT}$ – the helicopter detection range (radar 'Lis – 3(2)M', TT, 12 km [2]); $\sigma$, $\sigma_{TT}$ – the effective scattering surface (ESS) of the target and TT ($\sigma_{TT} = 2.5\ m^2$), respectively; $\Delta$ – the active noise interference power ratio (residuals of interference after appropriate compensation) to the radar channel intrinsic noise power (weak intensity 2 times, medium – 5 times, strong – 16 times and suppressive – $10^2$ times); $q, q_{SNR}$ – the signal to noise ratio (SNR) in the radar channel radar (taken in the calculations 4 times) and the SNR at which the operator conducts target detection (for 'excellent' – 4.9 times, 'good' – 6.2 times, 'satisfactory' – 8.1 times), respectively; $K$ – the coefficient that takes into account the angles of the antenna radar closure (varies from 0 to 1, in numerical modeling took 1).

The calculation results are shown in Fig. 1 with the sixth curve (dashed line, $D_{d6}(\sigma)$). We note a significant increase in the range of detection of targets by radar $D_{d6}(\sigma)$, relative to the detection by the personnel of ZU $D_{d1}(S) - D_{d5}(\xi_s)$. The seventh curve (dot-dashed line, $D_{d7}(\Delta)$) is plotted at the action of interference on the radar channel of the radar when $\sigma = 1\ m^2$. Even with suppressive interference ($\Delta = 10^2$ times) the detection range is ~ 2.4 km, which is a reasonably good result.

On the polygon tests basis [1, 11, 12], the values of various statistical probabilities of targets detection by ZU-23 $P_d(D, S, P_{mt})$ personnel with $P_{mt}$ and without missing targets $P_d(D, S)$, as well as the probabilities of correct detection by the mm wavelength range radars $P_d(D, \sigma, \Delta)$ [6] are equal:

$$P_d(D, S, P_{mt}) \approx (1 - P_{mt}) \exp\left\{-\left[(0.808\ D)/D_d(S)\right]^8\right\}$$
$$P_d(D, \sigma, \Delta) \approx F^{\left\{1/\left[1 + q(D, \sigma, \Delta)^2/2\right]\right\}} \tag{3}$$

where $F$ is the false alarm probability in the radio channel of the mm wavelength range radar [6] (taken according to the technical specifications on the radar $2 \times 10^{-3}$); the SNR in the radar channel, with $q(D, \sigma, \Delta) \approx 2\sqrt{(3.31 \times 10^{16}\ \sigma)/\left[D^4 (1 + \Delta)\right]}$.

The calculation results by expression (3) are shown in Fig. 2. The first curve $P_{d1}(D)$ (continuous line) and the second curve $P_{d2}(D)$ (dots line) depict the values of the statistical probability of ZU TT detection personnel when $S_{min\,TT} = 9.1\ m^2$ and UAV $S_{min\,F} = 0.58\ m^2$, with possible target miss $P_{mt} = 0.4$. We obtain $P_{d1}(6.8 \times 10^3) \approx 0.5$ and $P_{d1}(1717) \approx 0.5$.

Using the second formula from (3), we derived the third curve (dashed line) and the fourth curve (dot-dashed line). These curves represent the detection probability values of the helicopter by the mm-wave radar, both without interference and under strong interference, so $P_{d3}(12 \times 10^3) \approx 0.5$ and $P_{d4}(5914) \approx 0.5$ Note the high probability of airborne target detection by mm wavelength range radars.

Large-scale modeling of the ZU 23 mm projectiles ESS and the observation angle determination by the radar were conducted. The model samples included the 9M22, OF-462, and OF-25 projectiles in the decimeter and centimeter wavelength ranges [7, 8]. The radar wavelength calculation is determined using the following formulas [9]:

$$\lambda_d\left(\lambda_m, d_m\right)=\lambda_m \frac{d_{23}}{d_m}$$
$$\lambda_L\left(\lambda_m, L_m\right)=\lambda_m \frac{L_{23}}{L_m} \quad (4)$$

where $\lambda_d, \lambda_m$ – respectively, the wavelength for the radar by the caliber of the projectile and the mock-up; $d_m$, $d_{23}$ – the caliber of the mock-up and 23 mm projectile ($d_{23}=23\times10^{-3}$ m), respectively; $\lambda_L$ – the wavelength for the radar by the 23 mm projectile length; $L_m$, $L_{23}$ the mock-up length and 23 mm projectile, respectively ($L_{23}=0.106$ m).

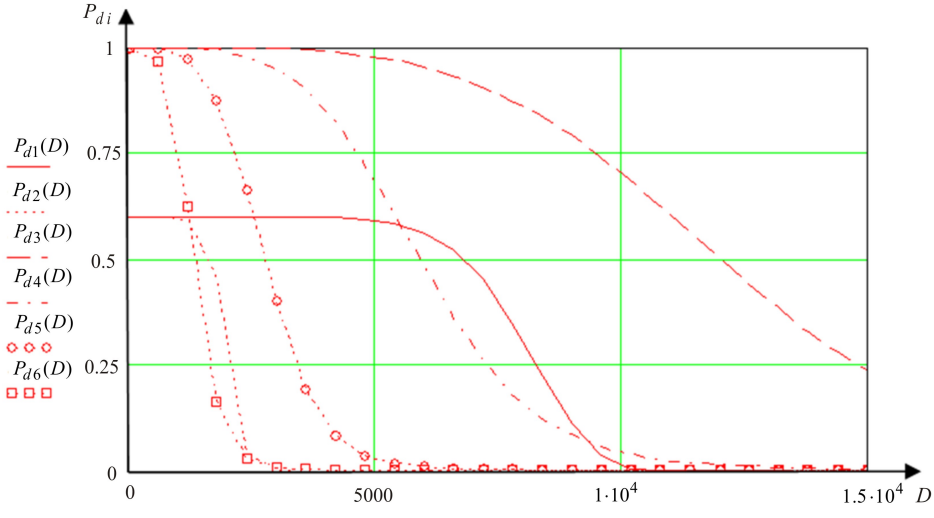


*Fig. 2 Statistical probabilities of detecting various targets by personnel operating ZU-23 and radar system $P_{di}(D)$ in relation to their distance D*

A good match was obtained at $\lambda_d \approx \lambda_L \approx 5.9$ mm (~ 50.56 GHz) on the OF-25 projectile. Besides, if the angle between the projectile axis and the standard to the radar antenna directional pattern (DP) is in the range from 0° to 45°, when the location angle $\varepsilon \approx 0°$, the projectile ESS $\sigma_{23} \approx 0.12$ m$^2$, and when $\varepsilon \approx 10°$, the projectile ESS $\sigma_{23} \approx 6.5\times10^{-3}$ m$^2$ [7, 8].

The angle between the projectile axis (Fig. 3), which is found on the flight path, and the normal to the radar antenna DP $\alpha(H, r_h, \beta_{TT})$ is equal to

$$d_h(H,\ r_h)=H/\tan\left[\arcsin\left(H/r_h\right)\right],$$
$$\gamma_h(\beta_{TT})=\beta_{rad}-\beta_{TT}$$
$$D(H,\ r_h,\ \beta_{TT})=\sqrt{B^2+d_h\left(H,\ r_h\right)^2-2B\,d_h\left(H,\ r_h\right)\cos\left[\gamma_h\left(\beta_{TT}\right)\right]+H^2} \quad (5)$$
$$\alpha(H,\ r_h,\ \beta_{TT})=\arccos\left[\frac{r_h^2+D\left(H, r_h,\ \beta_{TT}\right)^2-B^2}{2\,r_h\,D\left(H,\ r_h,\ \beta_{TT}\right)}\right]$$

where $d_h(H, r_h)$ – the horizontal range to the target (Fig. 3); $H, r_h$ – the target flight altitude and slant range to the far edge of the firing zone (FZO); $\beta_{TT}, \beta_{rad}$ – the azimuths of the target and radar relative to the direction to the North (22 → 11) (selected $\beta_{rad} = 2.7$ rad ); $D(H, r_h, \beta_{TT})$ – the slant range to the target from the radar; $B$ – the horizontal range between the ZU and the radar (in the modeling we took $B = 10^2$ m ).

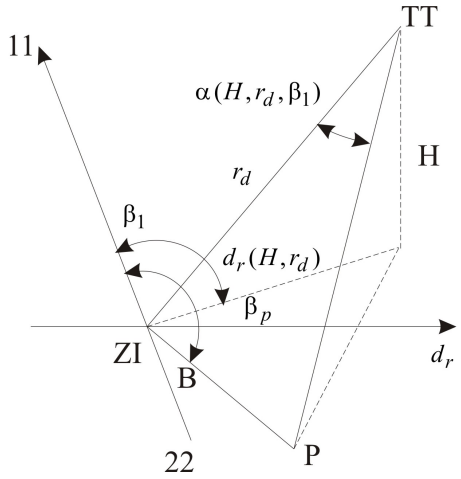


*Fig. 3 Determining the angle between projectile axis and the normal to the antenna's radiation pattern in radar system* $\alpha(H, r_h, \beta_{TT})$

The results of calculations $\alpha(H, r_h, \beta_{TT})$ are shown in Fig. 4. The first continuous curve $\alpha_1(H)$ is obtained while changing $H$ when $r_h = 2 \times 10^3$ m and $\beta_{TT} = 2.7$ rad. The second curve $\alpha_2(r_h)$ (··×··×··) and the third curve $\alpha_3(\beta_{TT})$ (points line) are respectively obtained at $H = 10^2$ m and $H = 10$ m, as $\beta_{TT} = 2.7$ rad, $r_h = 2 \times 10^3$ m. In order to analyze the curve course in Fig. 4, the fourth curve values $\alpha_4(\beta_{TT})$ (dashed line), and the fifth curve $\alpha_5(\beta_{TT})$ (dot-dashed line) are extended by 2° and 4°.

These curves were calculated when $H = 10^2$ m and $H = 10^3$ m at $r_h = 2 \times 10^3$ m. Typically, $\alpha(H, r_h, \beta_{TT})$ is lower than 2.9° (Fig. 4). We found that the reflected signal is primarily generated by the bottom slice of the projectile, where its effective scattering surface (ESS) can exceed approximately 0.12 m², depending on the projectile's angle of orientation [7, 8]. Curves five $P_{r5}(D)$ (··○··○··) and six $P_{r6}(D)$ (··□··□··) in Fig. 2 are plotted respectively when $\sigma_{23} \approx 0.12$ m$^2$ and $\sigma_{23} = 6.51 \times 10^{-3}$ m$^2$ ($\varepsilon \approx 10°$).This suggests the possibility of stable detection of a 23 mm projectile by a millimeter-wave radar (~5.9 mm) within the firing zone of the directional sounder at $\varepsilon \approx 0°$ $P_{d5}(2770) \approx 0.5$. When $\varepsilon \approx 10°$ the detection range is slightly reduced, so $P_{d6}(1336) \approx 0.5$. The obtained results create conditions for the detection of firing projectiles along the trace and the introduction of firing adjustments to improve its effectiveness.

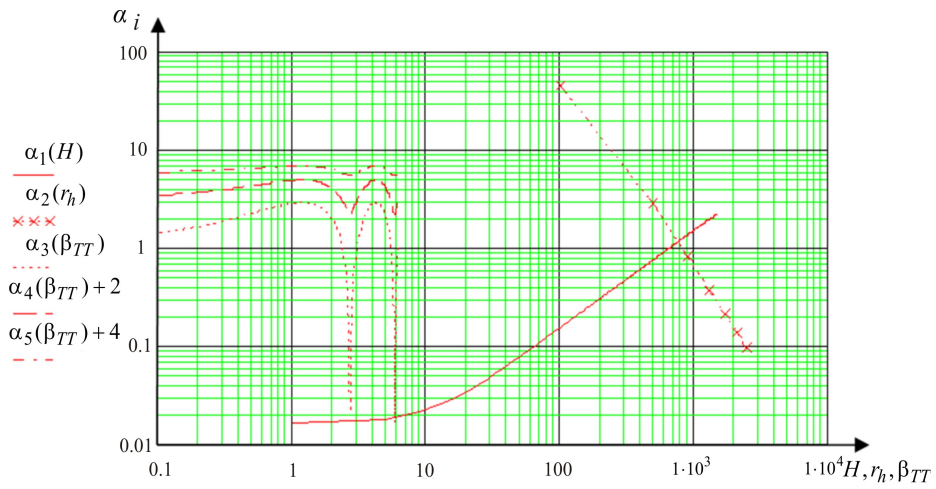


*Fig. 4 Angle values between projectile axis and the normal to the antenna's radiation pattern in radar system as they change the $H$, $r_h$, $\beta_{TT}$*

**Conditional probability of hitting the target at *n* shots** $R_n\left(S,\sigma_y,\sigma_z,r_y,r_z,\omega\right)$

The values $R_{ni}$ have been derived using the following expressions [4, 5]:

$$P_1\left(S,\sigma_y,\sigma_z,r_y,r_z\right)=\frac{S}{2\pi\sigma_y\sigma_z}\exp\left\{-0.5\left[\left(\frac{r_y}{\sigma_y}\right)^2+\left(\frac{r_z}{\sigma_z}\right)^2\right]\right\}$$

$$G\left(\omega\right)=1/\omega \tag{6}$$

$$R_1\left(S,\sigma_y,\sigma_z,r_y,r_z,\omega\right)=P_1\left(S,\sigma_y,\sigma_z,r_y,r_z,\omega\right)G\left(\omega\right)$$

$$R_n\left(S,\sigma_y,\sigma_z,r_y,r_z,\omega\right)=1-\left[1-R_1\left(S,\sigma_y,\sigma_z,r_y,r_z,\omega\right)\right]^n$$

where $P_{1j}$ – the hitting target probability in one shot; $\sigma_y,\sigma_z$ – the mean square deviations (MSD) of projectile firing errors (are within 25-50 m); $r_y,r_z$ – the systematic components in projectile firing; $G\left(\omega\right)$ – the probabilities of hitting the target when projectiles hit it $\omega$ ($\omega$ equal for TT from 2-6 projectiles, in modeling we took 4, for UAV – 1); $R_{1i}$, $R_{ni}$ – respectively, the probabilities of hitting the target in one shot and $n$ shots ($n=100$).

The calculation of projectile deviations in the firing plane, when shooting conditions deviate from standard values, was performed based on the principles of external ballistics for small-caliber anti-aircraft projectiles [4, 5, 10]. A solution matrix for the system of differential equations was employed using the Runge-Kutta method over the interval $t_2-t_1$ in MathCAD with a fixed step size of $n$. The initial time of projectile flight was $t_1=0$ s, and the final time was $t_2=5$ s. The number of steps within the interval when determining the root-mean-square deviation (RMSD) in range and altitude was set to 100.

Numerical simulations for one of the reference points at the ZU aim angle 1.5° at $D = 2$ km yielded a range $\sigma_d \approx 28$ m and altitude $\sigma_h \approx 3$ m RMS. However, in the firing tables [10], the RMSD values are for range $\sigma_d \approx 44.4$ m and altitude $\sigma_h \approx 2.4$ m, which indicates slightly improved values relative to the tabulated values. With this caveat, in the following we find approximate firing errors of the 23-mm twin ZU when firing at aerial targets, if the range is ~ 2 km or more.

Analyses of the firing errors magnitudes associated with projectile muzzle velocity, air density, projectile weight and wind have shown that projectile velocity and air density have the greatest influence on misses. On the basis of numerical modeling, the systematic components of the ZU-23 firing errors $r_i$ (with fragmentation, high-explosive, incendiary and tracer projectiles) along the $y$, $z$ axes in the picture plane were taken to be equal to $r_y \approx r_z \approx 60...20$ m.

The calculation results $R_{ni}$ according to (6) are shown in Fig. 5, when $\sigma_y \approx \sigma_z \approx 37$ m. The first line $R_{n1}(S)$ (continuous) and the second line $R_{n2}(S)$ (dots) are obtained by firing TTs ( $\omega$=4 ) and ZU ( $\omega$=1 ), at averaged $r_y \approx r_z \approx 40$ m values. The third straight line for TT $R_{n3}(S)$ (dash) and the fourth for UAV $R_{n4}(S)$ (dots and dashes) are plotted while pointing at targets behind the tracer tracks. Based on the experimental data, the systematic components can be reduced to $r_y \approx r_z \approx 20$ m. We note that the probabilities of hitting the target are not high at small target angles, so: $R_{n3}(9.1) \approx 0.02$ and only $R_{n4}(0.58) \approx 0.005$.

The slant range to the far edge of the sounder firing zone is $r_{di}$. If there are no angles of closure of the ZU firing position ( $K_c = 1$) and the target heading parameter is close to zero, the slant range to the ZU firing zone is denoted by $r_d(S, \xi_c, \xi_m, \xi_p, \xi_s, V)$. When the target designation (TD) from the mm range radar is worked out by the sounder personnel, we have the following slant range to the sounder's ZU $r_d(\sigma, \Delta)$.

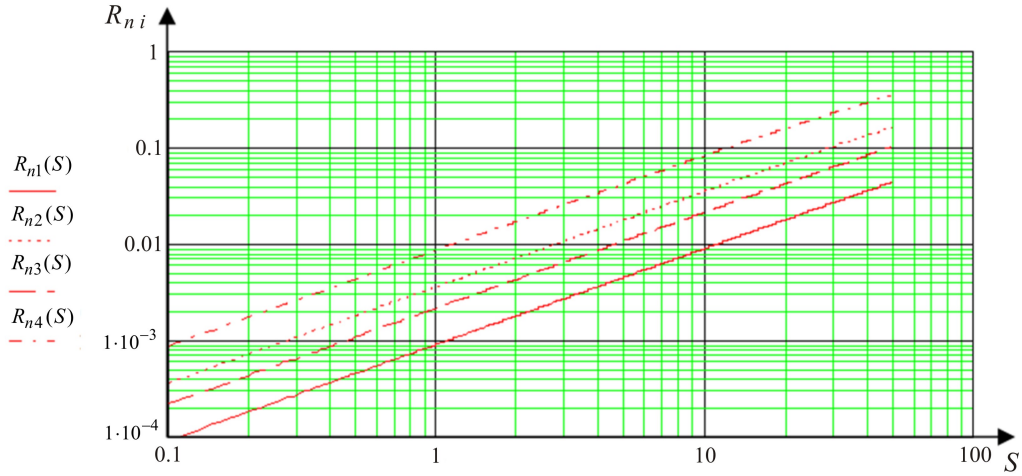


*Fig. 5 Conditional probabilities $R_{ni}$ of target engagement as a function of the S value in the firing plane of the ZU*

The slant ranges are calculated by the following expressions:

$$r_{\mathrm{d}}(S,\xi_c,\xi_m,\xi_p,\xi_s,K_{\mathrm{c}}) \approx \frac{D_{\mathrm{d}}(S,\xi_c,\xi_m,\xi_p,\xi_s,K_c) - V\left(\tau_{\mathrm{det}}+\tau_{\mathrm{inp}}\right)}{1+1.6\times 10^{-3}V} \quad \text{or}$$
$$r_{\mathrm{d}}(\sigma,\Delta) \approx \frac{D_{\mathrm{d}}(\sigma,\Delta) - V\left(\tau_{\mathrm{det}}+\tau_{\mathrm{inp}}\right)}{1+1.6\times 10^{-3}V} \tag{7}$$

where $V$ – the target flight speed (250 m/s was chosen for the TT, 40 m/s for the UAV); $\tau_{\mathrm{det}}$, $\tau_{\mathrm{inp}}$ – respectively, the time for determining and inputting input data (~ 3 s) and the time for assigning the type of fire (~ 2 s), taking into account the reaction time to signals and commands [1]; and $r_{\mathrm{d}}(S,\xi_c,\xi_m,\xi_p,\xi_s,V) \le 2.5$ km, and $r_{\mathrm{d}}(\sigma,\Delta) \le 2.5$ km.

The calculation results are shown in Fig. 6. The first curve $r_{\mathrm{d}1}(S)$ (continuous) is obtained by varying the target projection area $S$ in the firing picture plane. When $S > 4.5$ m$^2$, the introduced 2.5 km limit is triggered $r_{\mathrm{d}i}$. The Outpost UAV coloring effect is shown by the second curve $r_{\mathrm{d}2}(\xi_c)$ (dots line). When the color is not favorable ($\xi_c = 0.5$) and different MVR, a third curve $r_{\mathrm{d}3}(\xi_m)$ (··+··+··) is obtained. The fourth curve $r_{\mathrm{d}4}(\xi_p)$ (dots and dashes) shows the influence of the personnel ZU combat performance quality. Due to solar illumination, the range increases slightly, as the fifth curve $r_{\mathrm{d}5}(\xi_s)$ (··□··□··) illustrates. The sixth curve $r_{\mathrm{d}6}(V)$ (dashed line) indicates the values of the sounder firing zone $r_{di}$ depending on the UAV speed. We note a significant effect on the range $r_{\mathrm{d}i}$ of target detection by the naked eye $D_{\mathrm{d}i}$ (1).

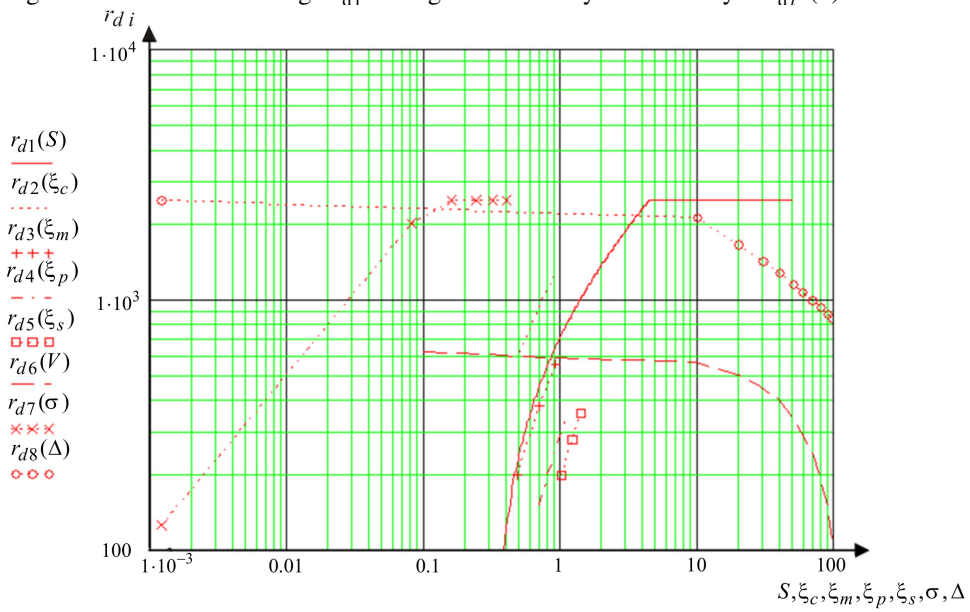


*Fig. 6 Slanted ranges to the far edge of the directional sounder firing zone* $r_{\mathrm{d}i}$

The seventh curve $r_{d7}(\sigma)$ $(\cdot\cdot\times\cdot\cdot\times\cdot\cdot)$ and the eighth curve $r_{d8}(\Delta)$ $(\cdot\cdot\circ\cdot\cdot\circ\cdot\cdot)$ are calculated using the second expression from (6). Working out the ZU TD personnel with mm range radars makes it possible to fire and small-sized targets with $\sigma \geq 10^{-2}$ m$^2$, so $r_{d7} \times (10^{-2}) \approx 840$ m. The influence of strong intensity interference (12 dB) on the radar radio channel slightly reduces the fire range – $r_{d8}(16) \approx 1.8 \times 10^3$ m. At present, remote control and firing ZU have been realized [11, 12]. The combined use of the sounder remote control and projectiles firing via the TD with the mm wavelength range radar gives advantages in terms of firing capabilities in various weather conditions at a greater distance.

Increase of ZU-23 firing efficiency when using target designation from mm wavelength radar $\Delta_i(D, \sigma, S, \omega)$.

The probability of ZU-23 firing task fulfilment when using TD with $P_{ft}(D, \sigma, S, \omega)$ and without radar is $P_0(D, S, \omega)$ [1, 4].

$$\begin{aligned} P_{ft}(D, \sigma, S, \omega) &= P_d(D, \sigma, \Delta) P_{per} P_{rel} R_n\left(S, \sigma_y, \sigma_z, r_y, r_z, \omega\right) \\ P_0(D, S, \omega) &= P_d(D, S, P_{mt}) P_{per} P_{rel} R_n\left(S, \sigma_y, \sigma_z, r_y, r_z, \omega\right) \\ \Delta(D, \sigma, S, \omega) &= [P_0(D, S, \omega) - P_{ft}(D, \sigma, S, \omega)] / P_{ft}(D, \sigma, S, \omega) \end{aligned} \tag{8}$$

where $P_{per}$, $P_{rel}$ – respectively, are the firing probabilities with average trained personnel (0.9) and the sounder reliability during preparation and firing (0.95).

In the modeling, the targeting behind the projectile paths was taken as $\sigma_y \approx \sigma_z \approx 37$ m, $r_y \approx r_z \approx 20$ m and $\omega = 4(1)$ for TT (UAV). For the TT operation, we obtained $P_{ft}(10^3; 1; 9.1; 4) \approx 1.7 \times 10^2$ and $P_0(10^3; 9.1; 4) \approx 10^{-2}$.

The results of calculations using the last expression from (8) are shown in Fig. 7.

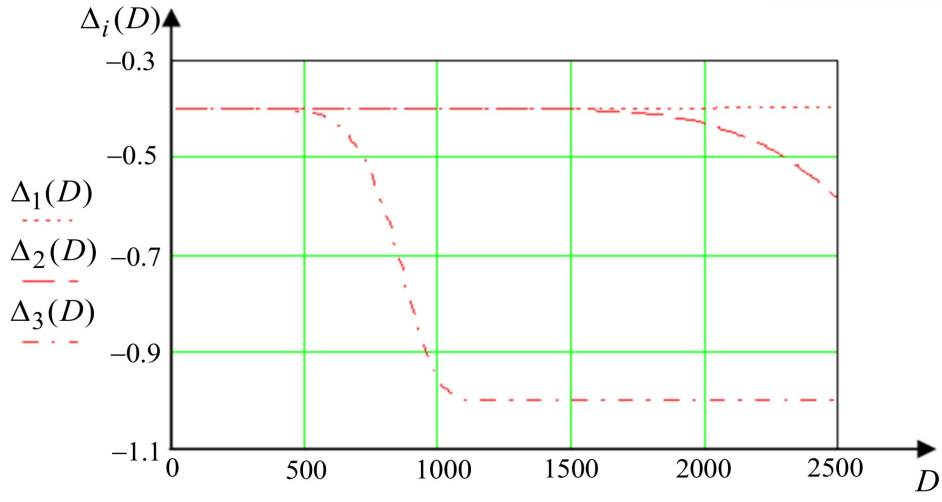


*Fig. 7 ZU-23 Increasing Firing Efficiency with Millimeter-Wave Radar Targeting* $\Delta_i(D)$

The first straight line $\Delta_1(D)$ (dots line) gives the increment in firing efficiency due to the radar TD using, while maintaining the TT – 0.4, and $\sigma = \sigma_{TT} = 1\ m^2$, $S = S_{min\ TT} = 9.1\ m^2$. The second curve $\Delta_2(D)$ (dashed line) and the third curve $\Delta_3(D)$ (dot-dashed line) represent the increase values in firing efficiency when operating on small targets. For the second curve $\sigma \approx 10^{-1}\ m^2$, $S \approx 1\ m^2$ and for the third curve $\sigma \approx 10^{-2}\ m^2$, $S \approx 10^{-1}\ m^2$. We obtained the following increments in firing efficiency $\Delta_2(2\times10^3) \approx -0.43$ and $\Delta_3(2\times10^3) \approx -1$. In general, the ZU remote control using with mm wavelength range radar increases the efficiency of firing projectiles from 0.4 to 1, which is a significant result of modeling.

It should also be noted that the usage of portable electronic tablets, the introduction of software with electronic tablets or smartphones would also improve the small-caliber weapons firing efficiency [13]. The typical target's own radiation usage, both in the audio wavelength range [14] and in the mm range [15, 16], will also lead to a TD quality increase on the ZU.

## 3 Conclusions

Therefore, it is proposed to enhance the effectiveness of engaging airborne targets by supplementing the ZU-23 system with millimeter-wave radar for target designation. To support this proposal, results from numerical modeling of target detection ranges and detection probabilities by ZU-23 personnel and millimeter-wave radar under various conditions are presented. An analysis of the conditional probability values for engaging various targets with the ZU-23 during firing was conducted. Slant range values to the far boundaries of the firing zones were determined for different combat conditions, considering parameters that reduce the conditional probability of target engagement.

Probabilities of successfully completing a fire mission with the ZU, both during autonomous operations and when receiving target designation from the millimeter-wave radar, were calculated. It is demonstrated that using millimeter-wave radar for target designation with the ZU-23 improves shooting effectiveness from 0.4 to 1. Additionally, suggestions for enhancing the performance indicators of ZU-23 firing are provided.

## References

[1] KOLOMIYTSEV, O., V. KUDRYASHOV and A. SHEVCHENKO. Effectiveness of Fire Control and Firing of a Portable Air Defense System Under the Specified Conditions of its Use (in Ukrainian). *Systems of Arms and Military Equipment*, 2009, **2**(18), pp. 14-16. ISSN 1997-9568.

[2] *RLS 'Lys-2M'* (in Ukrainian) [online]. 2023 [viewed 2023-02-09]. Available from: http://ust.com.ua/item/rls-lis-2m-2/

[3] *RLS 'Barsuk'* (in Ukrainian) [online]. 2023 [viewed 2023-02-09]. Available from: http://ust.com.ua/item/rls-barsuk-2/

[4] KONOVALOV, A. and Yu. NIKOLAEV. *External Ballistics* (in Russian) Moscow: Central Institute of Information, 1979.

[5] PISKUNOV, S., M. OBORONOV and O. KONOVALOV. Projectile Movement Model When Firing Anti-Aircraft Gun Systems (in Ukrainian). *Systems of Arms and Military Equipment*, 2009, **2**(18), pp. 28-32. ISSN 1997-9568.

[6] SHIRMAN, Y.D., ed. *Radio Electronic Systems. Fundamentals of Construction and Theory: Directory* (in Russian). 2nd ed. Moscow: Radiotekhnika, 2007. ISBN 978-5-88070-112-4.

[7] ZALEVSKY, G., O. SUKHAREVSKY, V. VASILETS and S. NECHITAYLO. Secondary Radiation of Resonance Perfectly Conducting Objects. *Journal of Communications Technology and Electronics*, 2014, **59**, pp. 1321-1332. DOI 10.1134/S1064226914100106.

[8] ZALEVSKY, G., O. SUKHAREVSKY, V. VASILETS and M. SURGAI. Estimation of Radar Scattering Characteristics of Artillery Shells in Meter, Decimeter and Centimeter Wavelength Ranges. *Radioelectronics and Communications Systems*, 2019, **62**(7), pp. 356-367. DOI 10.3103/ S0735272719070033.

[9] TROFIMOV, K.N., ed. Fundamentals of Radar. In: *Radar Reference Book* (in Russian). Moscow: SOV. RADIO, 1976.

[10] *Shooting Tables of the ZU-23 23-mm Twin Installation at Ground Targets. Fragmentation - High-Explosive - Incendiary Projectile* (in Russian). Moscow: VOENIZDAT, 1962.

[11] KUDRYASHOV, V., S. LEUSHYN and V. KONDRAT. Analysis of Possible Methods of Remote Control of the ZU-23-2 Taking into Account the Experience of the Anti-terrorist Operation in Eastern Ukraine (in Ukrainian). *Systems of Arms and Military Equipment*, 2017, **4**(52), pp. 38-45. ISSN 1997-9568.

[12] LEONOV, I., S. LESHCHENKO, V. KUDRYASHOV and S. LEUSHYN. Analysis of the Possibility of Automated Targeting of Small-Caliber Anti-Aircraft Artillery (in Ukrainian). *Scientific Works of Kharkiv National Air Force University*, 2019, **2**(60), pp. 91-98. ISSN 2073-7378.

[13] BALABUKHA, O., V. GREKOV and I. AKULENKO. Evaluation of the Effectiveness of the Combat Use of Means of Destruction, Taking into Account the Influence of the Technical Characteristics of Intelligence and Control Systems (in Ukrainian). *Scientific Works of the Armed Forces United Scientific Research Institute*, 2005, **2**(2), pp. 79-84.

[14] KUDRIASHOV, V. Improvement of Range Estimation with Microphone Array. *Cybernetics and Information Technologies*, 2017, **17**(1), pp. 113-125. DOI 10.1515/cait-2017-0009.

[15] LUKIN, K., V. KUDRIASHOV, P. VYPLAVIN and V. PALAMARCHUK. Coherent Imaging in the Range-Azimuth Plane Using a Bistatic Radiometer Based on Antennas with Beam Synthesizing. *IEEE Aerospace and Electronic Systems Magazine*, 2014, **29**(7), pp. 16-22. DOI 10.1109/MAES.2014.130142.

[16] LUKIN, K., V. KUDRIASHOV, P. VYPLAVIN, V. PALAMARCHUK and S. LUKIN. Coherent Radiometric Imaging Using Antennas with Beam Synthesizing. *International Journal of Microwave and Wireless Technologies*, 2015, 7(3-4), pp. 453-458. DOI 10.1017/ S1759078715000550.